



ELSEVIER

Available online at www.sciencedirect.com

SCIENCE @ DIRECT®

Journal of Sound and Vibration 285 (2005) 925–939

JOURNAL OF
SOUND AND
VIBRATION

www.elsevier.com/locate/jsvi

Natural vibration of arbitrary spatially curved rectangular rods with pre-twisted angles

Y.D. Shih^{a,*}, J.K. Chen^a, Y.C. Chang^a, J.P. Sheng^b

^a*Department of Mechanical Engineering, Tatung University, Taipei, Taiwan*

^b*Department of Civil Engineering, National Central University, Chung-li, Taiwan*

Received 28 July 2003; received in revised form 16 August 2004; accepted 10 September 2004

Available online 23 December 2004

Abstract

For the natural vibration of rods of pre-twisted rectangular cross-sections with its centerline spatially curved and twisted arbitrarily, a system of non-dimensional ordinary differential equations is obtained in three translation displacements and three rotational angles of the rod. The eigenvalue problem is solved for the natural frequencies of various pre-twisted angles of the rectangular cross-section area, aspect ratios, slenderness ratio, end conditions and functions of varying cross-section area along the rods by using a numerical method of Runge–Kutta integration. The eigenvalues are determined by the vanishing of a rank-six determinant whose column vectors are obtained at the end of six independent numerical integrations. The differential equations of the adjoint operator system for the eigenvalue problem with its associated boundary conditions are also derived and solved for the eigenvalues to check with that of the vibration system. It is found that the effect of increasing pre-twisted angle of the rod is that the lowest natural frequency of an arbitrary curved rod will asymptotically tend to be a constant, in spite of slenderness ratio, aspect ratio of the rectangular cross-section, E/G ratio, types of end conditions, or the functions of the cross-section area along the rod.

© 2004 Elsevier Ltd. All rights reserved.

*Corresponding author. Fax: +886 02 2599 714.

E-mail address: ydshih@ttu.edu.tw (Y.D. Shih).

Nomenclature			
ASPR	aspect ratio of the rectangular rod	PE	potential energy of a rod
a	radius of cylindrical surface for a helix	\vec{q}	internal force in the rod cross-section
b	pitch of helix divided by 2π	(Q_1, Q_2, Q_3)	components of amplitude of shear force \vec{q} for small oscillation
A_3, A_{30}	cross-section area of rod	S, s	non-dimensional and dimensional measurement along arc length
C_i	independent coefficients for $\vec{\Psi}_i$, $i = 1, \dots, 6$	T	non-dimensional torsion
d	diameter of a circular rod with its cross-section area equal to that of the rectangular rod	\bar{t}	a variable of parametric expression for the curve of rod geometry
$(\vec{e}_1, \vec{e}_2, \vec{e}_3)$	base unit vectors in principal normal, bi-normal and tangential directions	$\vec{u}, (u_1, u_2, u_3)$	displacement vector of rod element
E	Young's modulus	(U_1, U_2, U_3)	components of amplitude of displacement vector \vec{u} for small oscillation in x_1, x_2 , and x_3 directions
G	shear modulus	$(V_1, V_2, \dots, V_{12})$	components of amplitude of variables in adjoint operator system
$I_{11}, I_{22}, I_{33}, I_{12}, I_{10}, I_{20}$	dimensional moment of inertia	$\vec{x}, (x_1, x_2, x_3)$	local reference frame
I_1, I_2, I_{12}, I_3	non-dimensional moments of inertia, (dimensional I)/ $A_3\ell^2$	β	uniform pre-twist angle per unit arc length of the rod
$\vec{k}, (k_1, k_2, k_3)$	bending or twist rotational deformation	$\vec{\epsilon}$	stretching and shear deformation of rod element
K, Γ	non-dimensional curvatures	$\vec{\theta}$	rotation vector of rod element
KE	kinetic energy of rod	$(\Theta_1, \Theta_2, \Theta_3)$	components of amplitude of rotation vector $\vec{\theta}$ for small oscillation
L	lagrangian of a rod, $L = \text{KE} - \text{PE}$	κ, γ	dimensional curvatures, $\sqrt{\kappa^2 + \gamma^2} = a/(a^2 + b^2)$
ℓ	length of the rectangular rod	ρ	density
\vec{m}	internal moment in the rod cross section	τ	dimensional torsion, $b/(a^2 + b^2)$
(M_1, M_2, M_3)	components of amplitude of moment \vec{m} for small oscillation	$\vec{\Psi}$	variable vector of the system of linear differential equations
N	the matrix of the system of linear differential equations	Ω, ω	non-dimensional and dimensional angular frequency, $\Omega^2 = (\rho\ell^2/E)\omega^2$
Ω_1	the first lowest frequency of natural vibration	$(\Omega_1)_{\text{E.B.}}$	first lowest frequency Ω for the straight Euler–Bernoulli beam
$(\Omega_1)_{\text{E.B.}}$	the first lowest natural frequency for the straight Euler–Bernoulli beam theory		

1. Introduction

Spatially curved and twisted rods find applications in many engineering and architectural systems. Tabarrok et al. developed a finite element formulation for the free vibration of this type of rods [1], and also a computation method for the dynamics of these rods [2]. In the early days there has been a number works on the dynamics of planar rods [3–7], and on the pre-twisted, curved and helical rods [8–13]. In the related work on buckling of helical springs under compression and, or torsion, Yildirim [14] verified that the rod-model approximation is appropriate for springs with large numbers of turns. Recently, Tobarrok and Xiong [15] derived a finite element formulation for the

vibration and buckling of curved and twisted rods under load. Also, Cleghorn [16] studied the natural frequencies of helical spring subject to a static axial compression load by using transfer matrix method. In the present study, simple finite steps of integration of numerical calculation for a system of first-order ordinary differential equations and the boundary conditions are developed to obtain the nature frequencies of arbitrarily spatially curved rectangular pre-twisted rod, with its centerline being a space curve featured by varying space-curve curvature and torsion.

2. Formulation

The local coordinate reference frame x_1, x_2 and x_3 (principal normal ‘ \vec{e}_1 ’, bi-normal ‘ \vec{e}_2 ’ and tangent ‘ \vec{e}_3 ’ to the general helix) is used in the formulation of the differential equations. For the system as illustrated in Fig. 1, the arc length of the rod along its centerline is denoted by s , and κ, γ are the curvatures, τ is the torsion of the centerline. At each point of the centerline of the rod, one must define a local ortho-normal system of vectors in the Serret–Frenet formulas as in Ref. [17], they are

$$\begin{aligned} \frac{d\vec{e}_1}{ds} &= \tau\vec{e}_2 - \kappa\vec{e}_3, \\ \frac{d\vec{e}_2}{ds} &= -\tau\vec{e}_1 + \gamma\vec{e}_3, \\ \frac{d\vec{e}_3}{ds} &= \kappa\vec{e}_1 - \gamma\vec{e}_2. \end{aligned} \tag{1}$$

Let a rod of finite length subject to small deformation in stretching, shear and bending. The change in the rotation vector of a sliced cross-section element may be expressed as

$$\vec{k} = \frac{\partial \vec{\theta}}{\partial s}, \tag{2a}$$

where \vec{k} denotes the change in curvature–twist along the arc length s . For the stretching and shear deformations $\vec{\varepsilon}$, one can express the change in the displacement vector \vec{u} of a sliced cross-section element as

$$\vec{\varepsilon} = \frac{\partial \vec{u}}{\partial s} + \vec{e}_3 \times \vec{\theta}, \tag{2b}$$

where $\vec{\varepsilon}$ denotes the stretching and shear deformation. These two equations may be viewed as generalization of the Timoshenko beam kinematics to curved rods. For linearly elastic behavior, $\vec{\varepsilon}$ and \vec{k} may be written in the constitutive relations as

$$\vec{q} = \begin{bmatrix} GA_3 & 0 & 0 \\ 0 & GA_3 & 0 \\ 0 & 0 & EA_3 \end{bmatrix} \begin{bmatrix} \varepsilon_1 \\ \varepsilon_2 \\ \varepsilon_3 \end{bmatrix}, \tag{3}$$

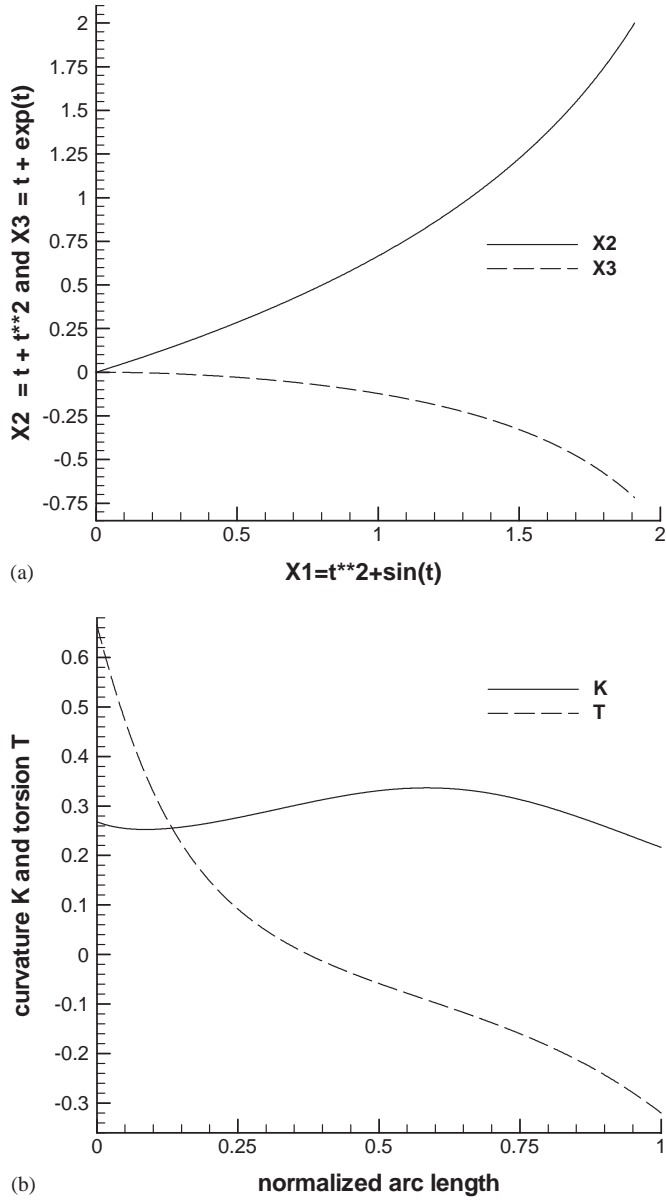


Fig. 1. (a) Space geometry and (b) curvature and torsion of the rod, for $\Gamma = 0$.

$$\vec{m} = \begin{bmatrix} EI_{11} & EI_{12} & 0 \\ EI_{21} & EI_{22} & 0 \\ 0 & 0 & GI_{33} \end{bmatrix} \begin{bmatrix} k_1 \\ k_2 \\ k_3 \end{bmatrix}, \tag{4a}$$

where \vec{q} and \vec{m} are the internal force and moment vectors in the rod. A_3 denotes the cross-section area of the rod. E and G denote Young's modulus and shear modulus, respectively. I_{11} , I_{12} , I_{21} , and I_{22} are

the element of the inertia tensor of area moment about the axes \vec{x}_1 and \vec{x}_2 , while I_{33} denotes the torsion constant. If the pre-twisted angle per unit length of the rod is β along the arc length s , and I_{10} and I_{20} denote the principle moment of inertia. Then, we have

$$\begin{aligned} I_{11} &= -I_{10} \cos^2(\beta s) + I_{20} \sin^2(\beta s), \\ I_{22} &= I_{10} \sin^2(\beta s) + I_{20} \cos^2(\beta s), \\ I_{12} &= -(I_{10} - I_{20}) \sin(\beta s) \cos(\beta s), \\ I_{21} &= I_{12}. \end{aligned} \tag{4b}$$

Under prescribed configuration of the rod, the potential energy PE and the kinetic energy KE of the rod may be expressed as

$$PE = \int_0^\ell \frac{1}{2} (\vec{e} \cdot \vec{q} + \vec{k} \cdot \vec{m}) ds \tag{5}$$

$$KE = \int_0^\ell \frac{1}{2} \left(\rho A_3 \frac{\partial u_j}{\partial t} \frac{\partial u_j}{\partial t} + \rho I_{ij} \frac{\partial \theta_i}{\partial t} \frac{\partial \theta_j}{\partial t} \right) ds. \tag{6}$$

In the case of small displacements and rotations about equilibrium, the Lagrangian can be obtained

$$L = KE - PE. \tag{7}$$

A direct application of Hamilton’s principle for the curved rod

$$\begin{aligned} \delta \int_0^t L dt = \delta \int_0^\ell ds \int_0^t dt L \left(u_1, u_2, u_3, \theta_1, \theta_2, \theta_3, \frac{\partial u_1}{\partial s}, \frac{\partial u_2}{\partial s}, \frac{\partial u_3}{\partial s}, \right. \\ \left. \frac{\partial \theta_1}{\partial s}, \frac{\partial \theta_2}{\partial s}, \frac{\partial \theta_3}{\partial s}, \frac{\partial u_1}{\partial t}, \frac{\partial u_2}{\partial t}, \frac{\partial u_3}{\partial t}, \frac{\partial \theta_1}{\partial t}, \frac{\partial \theta_2}{\partial t}, \frac{\partial \theta_3}{\partial t}, s, t \right) = 0. \end{aligned} \tag{8}$$

This provides the Euler–Lagrange equation [18].

$$\frac{\partial}{\partial t} \frac{\partial L}{\partial (\partial u_i / \partial t)} + \frac{\partial}{\partial s} \frac{\partial L}{\partial (\partial u_i / \partial s)} - \frac{\partial L}{\partial u_i} = 0, \quad i = 1, 2, 3, \tag{9}$$

$$\frac{\partial}{\partial t} \frac{\partial L}{\partial (\partial \theta_i / \partial t)} + \frac{\partial}{\partial s} \frac{\partial L}{\partial (\partial \theta_i / \partial s)} - \frac{\partial L}{\partial \theta_i} = 0, \quad i = 1, 2, 3. \tag{10}$$

Written in detail, Eqs. (1), (2), (9) and (10) are as follows:

$$\begin{aligned} \frac{\partial}{\partial t} \left(\rho A_3 \frac{\partial u_1}{\partial t} \right) - \frac{\partial q_1}{\partial s} + \tau q_2 - \kappa q_3 &= 0, \\ \frac{\partial}{\partial t} \left(\rho A_3 \frac{\partial u_2}{\partial t} \right) - \frac{\partial q_2}{\partial s} - \tau q_1 + \gamma q_3 &= 0, \\ \frac{\partial}{\partial t} \left(\rho A_3 \frac{\partial u_3}{\partial t} \right) - \frac{\partial q_3}{\partial s} + \kappa q_1 - \gamma q_2 &= 0, \end{aligned}$$

$$\begin{aligned} \frac{\partial}{\partial t} \left(\rho I_{11} \frac{\partial \theta_1}{\partial t} \right) + \rho \frac{\partial}{\partial t} \left(I_{12} \frac{\partial \theta_2}{\partial t} \right) - \frac{\partial m_1}{\partial s} + q_2 + \tau m_2 - \kappa m_3 &= 0, \\ \frac{\partial}{\partial t} \left(\rho I_{22} \frac{\partial \theta_2}{\partial t} \right) + \rho \frac{\partial}{\partial t} \left(I_{12} \frac{\partial \theta_1}{\partial t} \right) - \frac{\partial m_2}{\partial s} - q_1 + \tau m_1 + \gamma m_3 &= 0, \\ \frac{\partial}{\partial t} \left(\rho I_{33} \frac{\partial \theta_3}{\partial t} \right) - \frac{\partial m_3}{\partial s} + \kappa m_1 - \gamma m_2 &= 0, \end{aligned}$$

$$\begin{aligned} \frac{\partial u_1}{\partial s} - \tau u_2 + \kappa u_3 - \theta_2 &= \frac{q_1}{GA_3}, \\ \frac{\partial u_2}{\partial s} + \tau u_1 - \gamma u_3 + \theta_1 &= \frac{q_2}{GA_3}, \\ \frac{\partial u_3}{\partial s} - \kappa u_1 + \gamma u_2 &= \frac{q_3}{EA_3}, \end{aligned}$$

$$\begin{aligned} \frac{\partial \theta_1}{\partial s} - \tau \theta_2 + \kappa \theta_3 + \frac{I_{12}}{I_{11}} \left(\frac{\partial \theta_2}{\partial s} + \tau \theta_1 - \gamma \theta_3 \right) &= \frac{m_1}{EI_{11}}, \\ \frac{I_{12}}{I_{22}} \left(\frac{\partial \theta_1}{\partial s} - \tau \theta_2 + \kappa \theta_3 \right) + \frac{\partial \theta_2}{\partial s} + \tau \theta_1 - \gamma \theta_3 &= \frac{m_2}{EI_{22}}, \\ \frac{\partial \theta_3}{\partial s} - \kappa \theta_1 + \gamma \theta_2 &= \frac{m_3}{GI_{33}}. \end{aligned} \tag{11}$$

For static situation, $\partial(\cdot)/\partial t = 0$, these 12 equations of Eq. (11) can be reduced to static form and are agreed with those static differential equations obtained by Motterhead [8]. As one attempting to look for normal mode solutions in which all the displacements and rotations oscillate with the same frequency ω , thus one may assume

$$\begin{aligned} q_i &= \hat{Q}_i(s)e^{i\omega t}, \\ m_i &= \hat{M}_i(s)e^{i\omega t}, \\ u_i &= \hat{U}_i(s)e^{i\omega t}, \\ \theta_i &= \hat{\Theta}_i(s)e^{i\omega t}. \end{aligned} \tag{12}$$

To reach a system of non-dimensional first-order differential equations one may introduce

$$\begin{aligned} \widehat{Q}_i &= EA_3 Q_i^*, \quad \widehat{M}_i = EA_3 \ell M_i^*, \quad \widehat{U}_i = \ell U_i^*, \quad \widehat{\Theta}_i = \Theta_i^*, \quad A_3 = A_{30} A^*(s), \\ I_{ii} &= A_3 \ell^2 I_i^*, \quad I_{ij} = A_3 \ell^2 I_{ij}^*, \quad \omega = \sqrt{E/\rho \ell^2} \Omega^*, \\ s &= \ell s^*, \quad \kappa = (1/\ell) K^*, \quad \tau = (1/\ell) T^*, \quad \gamma = (1/\ell) \Gamma^*. \end{aligned} \tag{13}$$

By removing all the *s for simplicity, the non-dimensional equations are

$$\begin{aligned}
 \frac{dQ_1}{ds} - TQ_2 + KQ_3 + \Omega^2 U_1 &= 0, \\
 \frac{dQ_2}{ds} + TQ_1 - \Gamma Q_3 + \Omega^2 U_2 &= 0, \\
 \frac{dQ_3}{ds} - KQ_1 + \Gamma Q_2 + \Omega^2 U_3 &= 0, \\
 \\
 \frac{dM_1}{ds} - TM_2 + KM_3 - Q_2 + \Omega^2(I_1\theta_1 + I_{12}\theta_2) &= 0, \\
 \frac{dM_2}{ds} + TM_1 - \Gamma M_3 + Q_1 + \Omega^2(I_2\theta_2 + I_{12}\theta_1) &= 0, \\
 \frac{dM_3}{ds} - KM_1 + \Gamma M_2 + \Omega^2 I_3\theta_3 &= 0, \\
 \\
 \frac{dU_1}{ds} - TU_2 + KU_3 - \theta_2 &= Q_1 \left(\frac{E}{G}\right), \\
 \frac{dU_2}{ds} + TU_1 + \theta_1 - \Gamma U_3 &= Q_2 \left(\frac{E}{G}\right), \\
 \frac{dU_3}{ds} - KU_1 + \Gamma U_2 &= Q_3, \\
 \\
 \frac{d\theta_1}{ds} - T\theta_2 + K\theta_3 + \frac{I_{12}}{I_1} \left(\frac{d\theta_2}{ds} + T\theta_1 - \Gamma\theta_3\right) &= \frac{M_1}{I_1}, \\
 \frac{I_{12}}{I_2} \left(\frac{d\theta_1}{ds} - T\theta_2 + K\theta_3\right) + \frac{d\theta_2}{ds} + T\theta_1 - \Gamma\theta_3 &= \frac{M_2}{I_2}, \\
 \frac{d\theta_3}{ds} - K\theta_1 + \Gamma\theta_2 &= \frac{M_3}{I_3} \left(\frac{E}{G}\right).
 \end{aligned} \tag{14}$$

The end conditions commonly used in Eqs. (14) may be fixed, free, pinned or sliding-end conditions at $s = 0$ and 1 . For these variety end conditions, the following mathematical conditions should apply respectively, $U_1 = U_2 = U_3 = \theta_1 = \theta_2 = \theta_3 = 0$, for fixed end condition, $Q_1 = Q_2 = Q_3 = M_1 = M_2 = M_3 = 0$, for pinned end condition, $M_1 = M_2 = M_3 = U_1 = U_2 = U_3 = 0$, for free end condition, and $Q_1 = Q_2 = Q_3 = \theta_1 = \theta_2 = \theta_3 = 0$, for sliding end condition.

3. Method of solution

A fourth-order Runge–Kutta algorithm [19] of step-by-step integration for a system of first-order ordinary differential with initial conditions is employed in the computation. It is convenient

to rewrite Eq. (14) in the form

$$\frac{d\vec{\Psi}}{ds} = N\vec{\Psi}, \tag{15}$$

where $\vec{\Psi} = [Q_1, Q_2, Q_3, M_1, M_2, M_3, U_1, U_2, U_3, \Theta_1, \Theta_2, \Theta_3]^T$. To illustrate the method, the fixed–free end conditions of a cantilever rod are considered. Let $\vec{\Psi}_1, \vec{\Psi}_2, \vec{\Psi}_3, \vec{\Psi}_4, \vec{\Psi}_5$ and $\vec{\Psi}_6$ be the six independent solutions obtained through the integration of Eq. (15) satisfying the end conditions at $s = 0, U_1 = U_2 = U_3 = \Theta_1 = \Theta_2 = \Theta_3 = 0$, therefore the six corresponding initial conditions for the six independent solutions of the system of differential equations are, $\vec{\Psi}_1(0) = [1 \ 0 \ 0 \ 0 \ 0 \ 0 \ 0 \ 0 \ 0 \ 0 \ 0 \ 0]^T, \vec{\Psi}_2(0) = [0 \ 1 \ 0 \ 0 \ 0 \ 0 \ 0 \ 0 \ 0 \ 0 \ 0 \ 0]^T, \dots$ and $\vec{\Psi}_6(0) = [0 \ 0 \ 0 \ 0 \ 0 \ 1 \ 0 \ 0 \ 0 \ 0 \ 0 \ 0]^T$ respectively. Finally, the general solution of Eq. (15) satisfies the boundary condition at $s = 0$, must be the linear combination of the six independent solutions.

$$\vec{\Psi}(s) = C_1\vec{\Psi}_1(s) + C_2\vec{\Psi}_2(s) + C_3\vec{\Psi}_3(s) + C_4\vec{\Psi}_4(s) + C_5\vec{\Psi}_5(s) + C_6\vec{\Psi}_6(s). \tag{16}$$

Imposing the condition at the free end, $Q_1 = Q_2 = Q_3 = M_1 = M_2 = M_3 = 0$ at $s = 1$, one must demand that the six components of $\vec{\Psi}(1)$ to be zero, that is,

$$\Psi_i(1) = 0, \quad i = 1, 2, \dots, 6.$$

Hence the function of Ω for eigenvalue relation is

$$F(\Omega) = \begin{vmatrix} \Psi_{11}(1) & \Psi_{21}(1) & \dots & \Psi_{61}(1) \\ \Psi_{12}(1) & \Psi_{22}(1) & \dots & \Psi_{62}(1) \\ \dots & \dots & \dots & \dots \\ \Psi_{16}(1) & \Psi_{26}(1) & \dots & \Psi_{66}(1) \end{vmatrix} = 0, \tag{17}$$

where $\Psi_{ij}(1)$ is the j th component of $\vec{\Psi}_i(1)$.

For fixed values of Γ, E and G , and variable parameters $K, T, I_1, I_2, I_{12}, I_3$, and A_3 along arc length, the eigenvalue can be found by sequentially searching for the zeros of the characteristic equation (17), $F(\Omega) = 0$.

4. Adjoint operator system

The formal adjoint operator $L^*(\vec{\Phi})$ [20] associated with the operator of differential equation (15) $L(\vec{\Psi})$ and the boundary conditions can be written as

$$\int_0^1 \vec{\Phi}^T L(\vec{\Psi}) ds = [\dots]_0^1 + \int_0^1 \vec{\Psi}^T L^*(\vec{\Phi}) ds, \tag{18}$$

where $\vec{\Phi}^T = [V_1, V_2, V_3, \dots, V_{12}]$, $\vec{\Psi}^T = [Q_1, Q_2, Q_3, M_1, M_2, M_3, U_1, \dots, \Theta_3]$ and the system of differential equations for adjoint operator $L^*(\vec{\Phi})$ are as follows:

$$\begin{aligned} \frac{dV_1}{ds} &= TV_2 - KV_3 + V_5 - \left(\frac{E}{G}\right)V_7, \\ \frac{dV_2}{ds} &= -TV_1 + \Gamma V_3 - V_4 - \left(\frac{E}{G}\right)V_8, \\ \frac{dV_3}{ds} &= KV_1 - \Gamma V_2 - V_9, \\ \frac{dV_4}{ds} &= TV_5 - KV_6 - \left(\frac{V_{10}}{I_1}\right), \\ \frac{dV_5}{ds} &= -TV_4 + \Gamma V_6 - \left(\frac{V_{11}}{I_2}\right), \\ \frac{dV_6}{ds} &= KV_4 - \Gamma V_5 - \left(\frac{V_{12}}{I_3}\right)\left(\frac{E}{G}\right), \end{aligned}$$

$$\begin{aligned} \frac{dV_7}{ds} &= -KV_9 + TV_8 + \Omega^2 V_1, \\ \frac{dV_8}{ds} &= \Gamma V_9 - TV_7 + \Omega^2 V_2, \\ \frac{dV_9}{ds} &= -\Gamma V_8 + KV_7 + \Omega^2 V_3, \end{aligned}$$

$$\frac{dV_{10}}{ds} = \left(\begin{array}{l} \left(-KV_{12} + TV_{11} + V_8 + \Omega^2(I_1 V_4 + I_{12} V_5) + \left(\frac{I_{12}}{I_1}\right)TV_{10} - V_{11} \frac{d}{ds} \left(\frac{I_{12}}{I_2}\right) \right) \\ - \left(\frac{I_{12}}{I_2}\right) \left(\Gamma V_{12} - TV_{10} - V_7 + \Omega^2(I_2 V_5 + I_{12} V_4) - \left(\frac{I_{12}}{I_2}\right)TV_{11} - V_{10} \frac{d}{ds} \left(\frac{I_{12}}{I_1}\right) \right) \end{array} \right) / \left(1 - \frac{I_{12}^2}{I_2 I_1} \right),$$

$$\begin{aligned} \frac{dV_{11}}{ds} &= \Gamma V_{12} - TV_{10} - V_7 + \Omega^2(I_2 V_5 + I_{12} V_4) - \left(\frac{I_{12}}{I_2}\right)TV_{11} - V_{10} \frac{d}{ds} \left(\frac{I_{12}}{I_1}\right) - \left(\frac{I_{12}}{I_1}\right) \frac{dV_{10}}{ds}, \\ \frac{dV_{12}}{ds} &= -\Gamma V_{11} + KV_{10} + \Omega^2 I_3 V_6 - I_{12} \left(\left(\frac{\Gamma}{I_1}\right) V_{10} - \left(\frac{K}{I_2}\right) V_{11} \right). \end{aligned} \tag{19}$$

For instance, the boundary condition for $\vec{V}(s)$ associated with a rod of ends fixed will be $V_1(s) = V_2(s) = V_3(s) = V_4(s) = V_5(s) = V_6(s) = 0$, at $s = 0$ and 1. Both the differential system of the rod vibration and its adjoint operator system are calculated to check the frequency in each other.

5. Results and discussions

In arriving the non-dimensional Eqs. (14), the dimension in angular velocity is in a form $\sqrt{E/\rho\ell^2}$ rather than $\sqrt{(E/\rho\ell^2)(I_1/A_3\ell^2)}$ as in the Euler–Bernoulli beam theory. The choice of the dimensional reference in present work comes from the fact that there are involved four distinct moments of inertia $I_1, I_2, I_{12},$ and I_3 in the problem instead of only one moment of inertia I_1 with respect to x_1 axes to be involved. The characteristic dimension for curvature and torsion is introduced by $1/\ell$. It can be interpreted that the physical quantity such as curvature can be considered as an accumulating quantity along the arc length.

For common end conditions of the rods there are two physical properties out of four in $\vec{Q}, \vec{M}, \vec{U},$ and $\vec{\Theta}$, to be set zero at $s = 0$ and 1. However, there are two combinations of the mathematical conditions, $\vec{Q} = \vec{U} = 0$ and $\vec{M} = \vec{\Theta} = 0$, not available due to lack of possible physical application. All computations are made for two systems of differential equations; one is the differential equation (15) and the related boundary conditions, while the other one is the adjoint operator system of the differential equation (18) and its corresponding adjoint boundary conditions. Mathematically, identical characteristic equations must obtain for these two systems. The eigenvalues are checked in each other to fulfill the criterion for required computation accuracy up to six decimal points.

First of all, Fig. 1(a) shows the geometry of an arbitrary space curve of the rod, which has a parametrical expression as $x_1 = \bar{t}^2 + \sin(\bar{t}), x_2 = \bar{t} + \bar{t}^2$ and $x_3 = \bar{t} + \exp(\bar{t})$, and its curvature and torsion along arc length s obtained through analytical differentiation are depicted in Fig. 1(b). In Fig. 2, the lowest four natural frequencies are plotted versus the pre-twisted angle of the

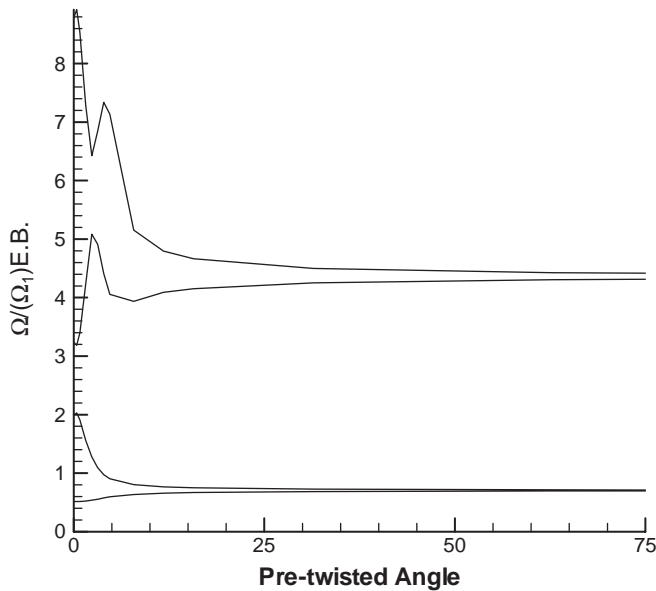


Fig. 2. The lowest four natural frequencies versus the varying pre-twisted angles for a cantilever rectangular rod of $ASPR = 2, E/G = 2.6,$ and $d/\ell = 0.01.$

rectangular cross-section area of the rod. The first frequency increases and the second frequency decreases monotonically against the pre-twisted angle, respectively, and meet each other asymptotically, while the third frequency increases and the fourth frequency decreases, they look like to be met and to be crossed each other at the pre-twist angle around 2.35. The lowest frequencies for three types of end condition of the rod, fixed–pinned, fixed–free, and fixed–fixed, versus the pre-twisted angles are shown in Fig. 3. For the fixed–free end condition, the lowest frequency varies with the pre-twisted angle smoothly, while for the end conditions fixed–pinned and fixed–free, the lowest frequency varies with the pre-twisted angle at several discontinuous slopes. As the pre-twisted angle becomes large, the effect of boundary conditions disappears. The frequencies converge to a same value. It is shown in Fig. 4 that if the cross section area of the rod is kept unchanged, the pre-twisted angle will not affect the natural frequency at aspect ratio equal to one, but the effect of pre-twisted angle will become to be saturated at a pre-twisted angle around 20 for aspect ratios 2, 4, and 8. The lowest natural frequency for two slenderness ratios of a rod is shown in Fig. 5. As the pre-twisted angle is greater than 20, there is only slight variations on the value of the lowest frequency. It takes note in Figs. 2, 3, and 5, that big changes in the frequencies of the rod at small pre-twisted angles less than 2 are observed in the result. The variation of the lowest natural frequency for three types of function of the cross section area along the rod is depicted in Fig. 6. Suppose one reshapes a uniform rectangular cross-section rod of aspect ratio 4 in such a way that the cross section area varies along the arc length as a linear or quadratic function, the natural frequency is raised about $\frac{1}{3}$ for large pre-twisted angles. The increase of the power in the non-uniformity function of cross-section area will push the natural frequencies up to a higher value. In Fig. 7, it is presented the effect of E/G ratio on the lowest frequency of the rod with pre-twisted angle varying. It is found that, as the pre-twisted angle is less

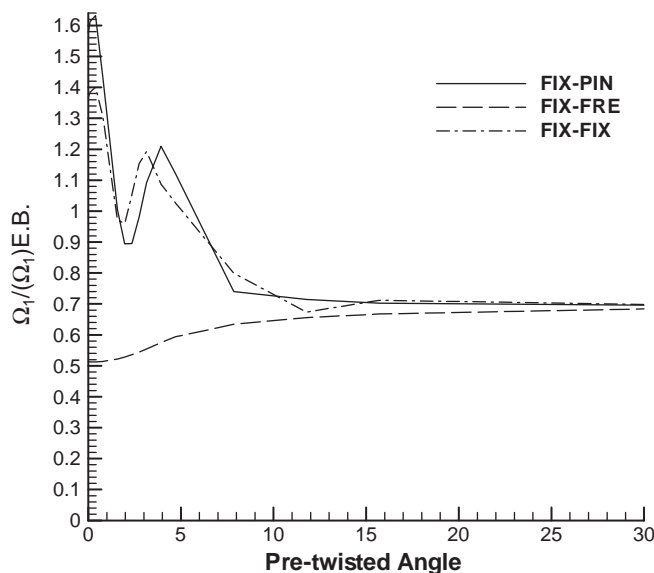


Fig. 3. The lowest natural frequency varying versus the pre-twisted angles for a rectangular rod of aspect ratio 4, $E/G = 2.6$, and $d/\ell = 0.01$ with three types of end conditions, fixed–pinned, fixed–free, and fixed–fixed.

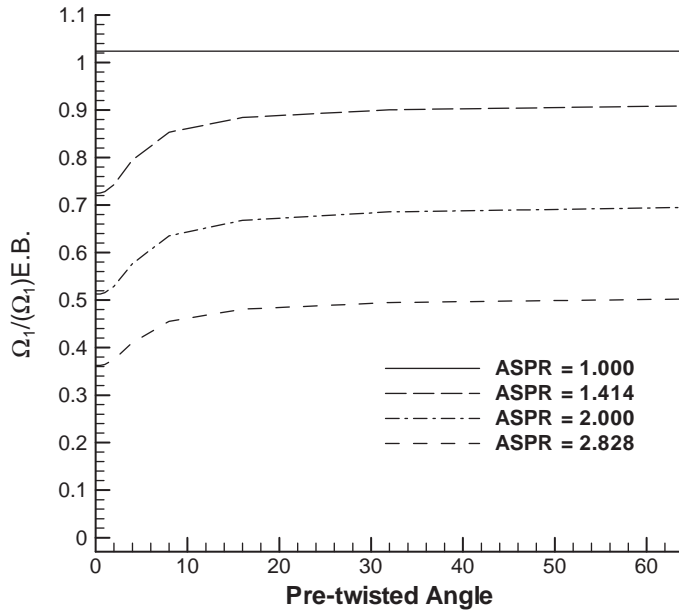


Fig. 4. The lowest natural frequency varying versus the pre-twisted angles for a cantilever rectangular rod of $E/G = 2.6$, and $d/\ell = 0.01$ with four aspect ratios, $ASPR = 1, 1.414, 2,$ and 2.828 , the cross-section area remained constant.

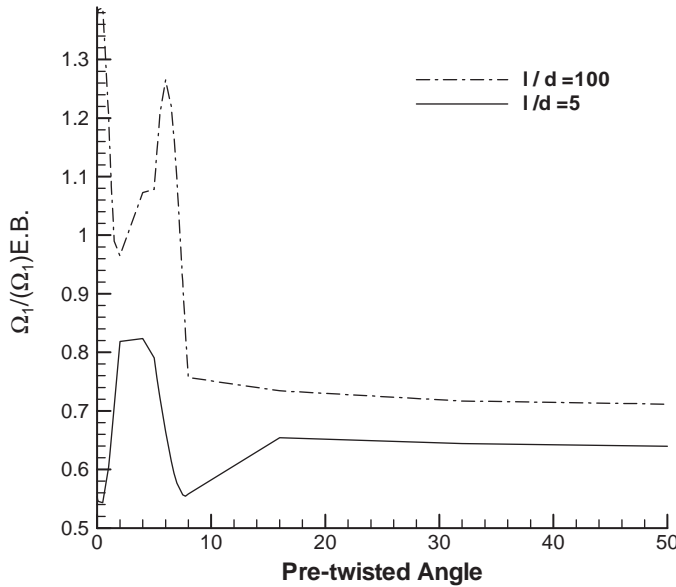


Fig. 5. The lowest natural frequency varying versus the pre-twisted angles for a both-end-clamped rectangular rod of $E/G = 2.6$, and aspect ratio = 4 with two slenderness aspect ratios, $d/\ell = 0.01$ and $d/\ell = 0.2$.

than 10, the lowest natural frequency for these two E/G ratios are not distinguishable. As the pre-twisted angle is greater than 20, a rod with less E/G ratio will give a higher natural frequency as expected. This agrees with the case if we consider no shear deformation, that is as G tends to

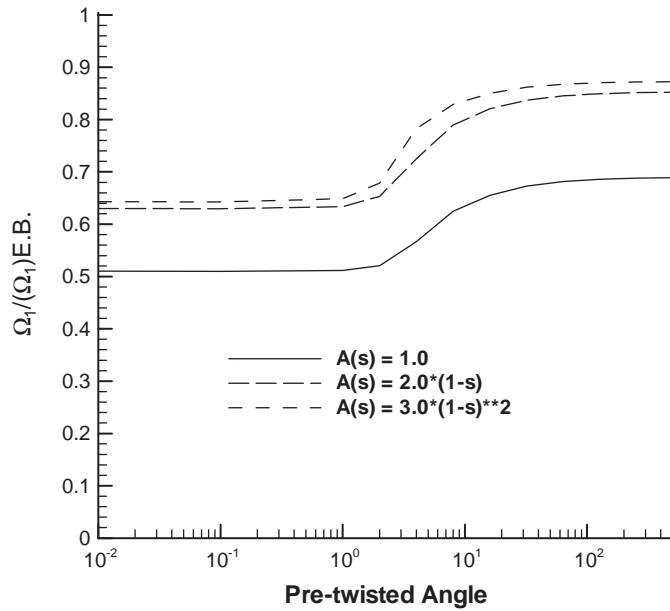


Fig. 6. The lowest natural frequency varying versus the pre-twisted angles for a cantilever rectangular rod of $E/G = 2.6, d/\ell = 0.2$ and aspect ratio = 4 with three variable cross-section areas, the total volume remained constant.

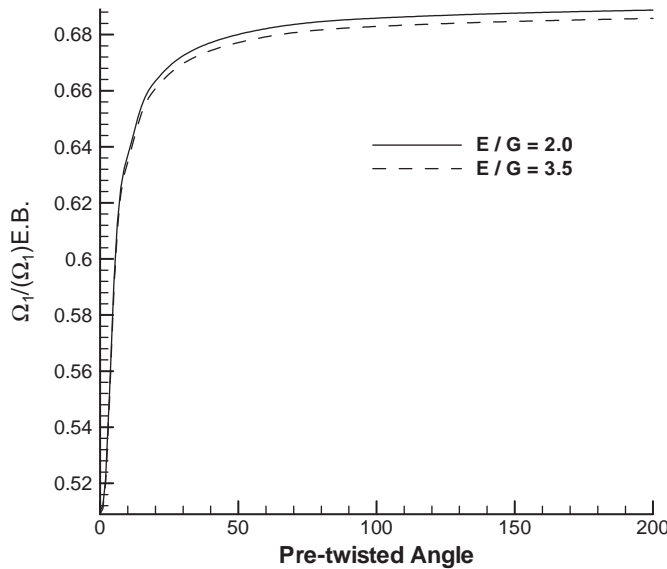


Fig. 7. The lowest natural frequency varying versus the pre-twisted angles for a cantilever rectangular rod of slenderness ratio $d/\ell = 0.2$ and aspect ratio $ASPR = 2$ with two E/G ratios equal to 2.0 and 3.5.

infinity, and there will be a higher natural frequency. Finally, the cross-section area of $ASPR = 1.414$ is cut from the x_1 normal axes, and pulled apart for a gap distance but linked by a rib of negligible mass. The lowest frequency varies along with the increase of pre-twisted angle is shown

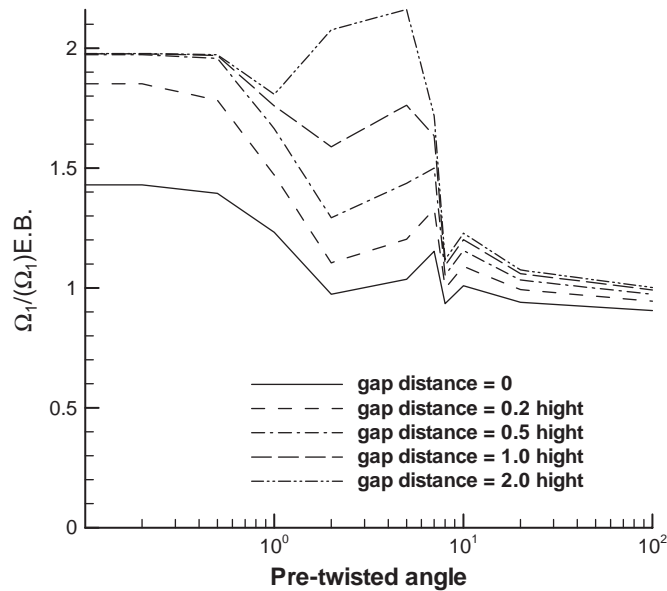


Fig. 8. The lowest natural frequency varying versus the pre-twisted angles for a both-end-fixed uniform rectangular rod of slenderness ratio $d/\ell = 0.01$, aspect ratio $ASPR = 1.414$ and E/G ratio equal to 2.6 with five gap distances.

in Fig. 8. It is observed that the lowest frequencies for various distance gaps will converge, as the pre-twisted angle tends to be large. Also, for a prescribed pre-twisted angle there is always a higher lowest frequency for a rod with higher gap distance.

6. Conclusion

The nature frequency of vibration for arbitrarily specified spatially curved rectangular rod, with the cross section area pre-twisted along the centerline of the rod, was studied together with the associated adjoint system by using a method of Runge–Kutta numerical integration. The constantly increased pre-twisted angle of a rod will finally make the lowest natural frequency to be saturated, in spite of the variations of slenderness ratio, aspect ratio of the rectangular cross-section, E/G ratio, types of end conditions, or the functions of the cross-section area along the rod.

References

- [1] B. Tabarrok, A.M. Sinclair, M. Farshad, H. Yi, On the dynamics of spatially curved and twisted rods—a finite element formulation, *Journal of Sound and Vibration* 123 (1988) 315–326.
- [2] B. Tabarrok, M. Farshad, H. Yi, Finite element formulation of spatially curved and twisted rods, *Computer Methods in Applied Mechanics and Engineering* 70 (1988) 275–299.
- [3] R. Davis, R.D. Henshell, G.B. Warburton, Constant curvature beam finite elements for in-plane vibration, *Journal of Sound and Vibration* 25 (1972) 561–576.

- [4] T.M. Wang, A.J. Laskey, M.F. Ahmad, Natural frequencies for out-of-plane vibrations of continuous curved beams considering shear and rotary inertia, *International Journal of Solids and Structures* 20 (1984) 257–265.
- [5] W.L. Cleghorn, B. Tabarrok, T.W. Lee, Vibration of rings with unsymmetrical cross-sections: a finite element approach, *Journal of Sound and Vibration* 168 (1993) 93–113.
- [6] E. Dokumaci, Pre-twisted beam elements based on approximation of displacements in fixed directions, *Journal of Sound and Vibration* 52 (1977) 277–282.
- [7] W.P. Howson, A.K. Jemah, Exact dynamic stiffness method for planar natural frequencies of curved Timoshenko beams, *Proceedings of the Institution of Mechanical Engineers* 213 (Part C) (1999) 687–696.
- [8] J.E. Mottershead, Finite elements for dynamical analysis of helical rods, *International Journal of Mechanical Sciences* 22 (1980) 267–283.
- [9] J.E. Mottershead, The large displacements and dynamic stability of springs using helical finite elements, *International Journal of Mechanical Sciences* 24 (1982) 547–558.
- [10] K. Nagaya, S. Takeda, Y. Nakata, Vibration of coil springs with arbitrary shape, *JSME* 51 (Part C) (1984) 3014–3021.
- [11] H. Nakamura, K. Suzuki, S. Shikanai, Accurate vibration analysis of a combined system consisting of multiple curved and straight bars (out-of-plane vibration), *JSME* 65 (Part C) (1998) 2168–2174.
- [12] H.S. Tsay, H.B. Kingsbury, Vibrations of rods with general space curvature, *Journal of Sound and Vibration* 124 (1988) 539–554.
- [13] V. Yildirim, N. Ince, Natural frequencies of helical spring of arbitrary shape, *Journal of Sound and Vibration* 204 (1997) 311–329.
- [14] G.G. Chassie, L.E. Becker, W.L. Cleghorn, On the buckling of helical springs under combined compression and torsion, *International Journal of Mechanical Sciences* 39 (1997) 697–704.
- [15] Y. Xiong, B.A. Tabarrok, A finite element model for the vibration of spatial rods under various applied loads, *International Journal of Mechanical Sciences* 34 (1992) 41–51.
- [16] L.E. Becker, G.G. Chassie, W.L. Cleghorn, On the natural frequencies of helical compression springs, *International Journal of Mechanical Sciences* 44 (2002) 825–841.
- [17] K. Nishinari, A discrete model of an extensible string in three-dimensional space, *Journal of Applied Mechanics* 66 (1999) 695–701.
- [18] F. Hildebrand, *Methods of Applied Mathematics*, Prentice-Hall, Englewood Cliffs, New Jersey, 1965, pp. 135–139.
- [19] B. Carnahan B, H. Luther, J. Wilkes, *Applied Numerical Methods*, Wiley, New York, 1969, pp. 363–368.
- [20] M.D. Greenberg, *Application of Green's Functions in Science and Engineering*, Prentice-Hall, Englewood Cliffs, NJ, 1971, pp. 56–59.